Geomechanics and Engineering, *Vol. 27, No. 1 (2021) 31-43*
https://doi.org/10.12989/gae.2021.27.1.031

Force change of the gravel side support during gangue heaping under a new non-pillar-mining approach

Jianning Liu[1,2,3a], Manchao He[1b], Shilin Hou[1c], Zhen Zhu[*1,4], Yanjun Wang[2d] and Jun Yang[1e]

[1]*State Key Laboratory for Geomechanics and Deep Underground Engineering, China University of Mining and Technology - Beijing, Beijing, 100083, China*
[2]*ShanXiYinFeng S&T CO., LTD, Taiyuan, 030000, China*
[3]*Department of Civil and Environmental Engineering, Universitat Politècnica de Catalunya, Barcelona Tech, 08034, Spain*
[4]*School of Civil Engineering, Qingdao University of Technology, Qingdao, 266033, China*

(Received August 8, 2020, Revised August 9, 2021, Accepted September 28, 2021)

Abstract. The force change characteristics of gravel side support structures during gangue heaping can provide useful information about roadway stability in a new non-pillar-mining approach—noncoal pillar mining with automatically formed gob-side entry (NMAFG). Considering the dynamic shock and static stacking phenomena during gangue heaping, the coefficient of restitution and Janssen model are introduced into the theoretical analysis. Analytical results show that the impact force decreased with increasing gangue heaping height under dynamic shock, while under static stacking, the gangue extrusion force first increased sharply, then increased slowly and stabilized, and the final force was unrelated to the gangue heaping height. Field monitoring was conducted to verify the rationality of the pattern obtained from theoretical analysis. The gangue support structure lateral stress from field monitoring can be divided into two periods. In Period I, the peak value at the lower monitoring point was greater than that at any other point. The lowest sensor was subjected to the greatest impact, at 59.09 kN. In Period II, the stress value first rapidly increased, then slowly increased and stabilized. The final force was unrelated to the gangue height. The sensors at #2 (highest position), #4 (middle position), and #6 (lowest position) measured 31.91 kN, 44.82 kN and 38.19 kN, respectively. The analysis confirmed the variation characteristics of the impact force and extrusion force.

Keywords: extrusion force; gangue heaping; impact force; non-pillar-mining approach

1. Introduction

Coal has always represented the majority of the energy structure in China. In coal mining, the traditional practice of long-wall mining is still applied today. However, increasing mining intensity and depth have exposed resource waste and the frequent occurrence of safety accidents as a result of traditional long-wall mining (Wojtecki *et al.* 2016, Hosseini 2017, Zhang *et al*. 2017, Konicek and Schreiber 2018, He *et al*. 2021). With respect to these problems, the practice of conventional gob-side entry retention (CGSER) has become a research focus in the field of coal mining, and this mining method can reduce roadway excavation and remove protective pillars (Zhang *et al*. 2015, Tan *et al*. 2019, Yang *et al*. 2020, Liu *et al*. 2021). In CGSER, insufficient caving of the gob-side roof results in a thicker hanging roof, and the pressure of the roadway is high. CGSER has difficulty sustaining the stability of the roadway structure. Considering the many problems in CGSER, the technique of noncoal pillar mining with automatically formed gob-side entry (NMAFGE) proposed by Academician Manchao He in 2009 can reduce roadway excavation by half, remove protective pillars, and effectively control some of the dynamic pressure disasters in entries (He *et al*. 2021). Based on the proven successful work of traditional NMAFGE, Academician Manchao He updated the NMAFGE method in 2016. This technique cuts the entry space with a coal cutter and eliminates roadway excavation, leading to a significant improvement in mining efficiency (Liu *et al*. 2019, He *et al*. 2021). NMAFGE still represents a significant underground space technology in coal mining.

In the NMAFGE experiment, the gob was the site of the heaping of gangue, which was then compressed. Therefore, the gravel side support in the experiment needs to experience the influence of the gangue accumulation and gangue compression processes. With respect to the force and stability analysis of the gangue support structure, some scholars have focused only on the force applied to the gangue support structure during gangue compaction (He *et al*. 2017, Zhen *et al*. 2019). The gangue heaping process should also be fully considered in studying the stress characteristics of gangue support structures. In the gangue heaping process, the gangue is likely to slide into the roadway if the stability of the gangue support structure is not sufficient, which may impose serious consequences for the evaluation of the support effect and the stability of the entry. Thus, the analysis of force change characteristics in the gangue support structure during gangue heaping is crucial to the stability of the gob-side entry. In recent years, some scholars have begun to analyse the force change characteristics of gangue support structures during gangue heaping (Hu *et al*. 2019, Zhang *et al*. 2020). However, these

*Corresponding author, Ph.D.
E-mail: zhuzhen@qut.edu.cn

ISSN: 2005-307X (Print), 2092-6219 (Online)

studies only analyse the patterns of numerical simulation and field monitoring data and lack more in-depth analysis and research on the gangue heaping process.

During the gangue heaping process, the gangue in gob will inevitably collide and undergo squeezing in the process of interaction. The gangue collision phenomenon is similar to a rockfall, which is a dynamic contact problem. For rockfall problems, the current mainstream analysis direction is coefficient of restitution research, which is a method to analyse the relationship between the velocity and trajectory before and after a collision (Sarfarazi *et al*. 2016, Gao and Meguid 2018, Nakajima *et al*. 2020). This paper introduces the collision coefficient to analyse the phenomenon of gangue collision on the side of the gangue support structure. The accumulation and extrusion process of the gangue at the side of the gangue support structure is similar to that of barn or mine bins. The Janssen model is the main method used for studying the force of granules in the accumulation of barn or mine bins. This model is based on the continuum model, and it is concluded that due to interactions between particles, the force in the direction of gravity is decomposed into the horizontal direction, and the sidewall supports part of the weight of the particles, making the pressure at the bottom tend to be saturated (Horabik *et al*. 2016, Matchett *et al*. 2018, Cisneros *et al*. 2020, Mahajan *et al*. 2020, Yoon *et al*. 2020, Zidek *et al*. 2020). However, the Janssen model is applicable to particles with an accumulation height of approximately more than two times the bottom diameter as the research object. In the NMAFGE experiment, the gangue lumpiness at the retaining side was less than 1 m, and the accumulation height was much more than twice the lumpiness. Therefore, the Janssen model can be introduced to study the force change characteristics of the gangue support structure during gangue heaping.

The research in this paper was performed as part of the NMAFGE experiment in the Ningtiaota Coal Mine. The distribution characteristics of the gangue beside the gangue support structure are divided into a dynamic shock phenomenon and a static stacking phenomenon. The forces applied to the gangue support structure were divided into an impact force and an extrusion force. For impact force analysis, the plane gangue collision mechanical model was constructed according to the impulse pattern and the coefficient of restitution. For extrusion force analysis, the plane gangue extrusion mechanical model was constructed in combination with the Janssen model. The evolution of the impact force and extrusion force applied to the gangue support structure was summarized. Field monitoring of the lateral stress applied to the gangue support structure was conducted, and image data on the deformation of the gangue support structure in the experiment were collected. The results obtained from the experiment validated the pattern of evolution of the impact force and extrusion force applied to the gangue support structure.

2. Project background

2.1 Overview of the experimental project

The NMAFGE experiment was successfully performed in the Ningtiaota Coal Mine. The Ningtiaota Coal Mine is located in northern Shaanxi Province on the Loess Plateau. The working face selected for the experiment was S1201-II. This region features an approximately horizontal coal seam, shallow burial depth and simple geological conditions. The design parameters of the NMAFGE experiment are shown in Fig. 1.

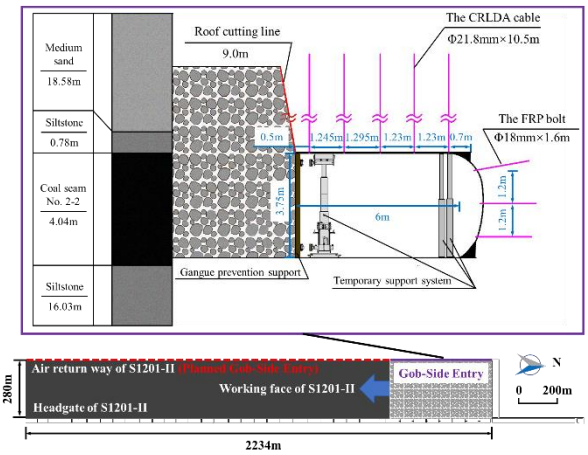

Fig. 1 Design parameters of the NMAFGE experiment (Liu *et al*. 2019)

As shown in Fig. 2, the main support system and basic support equipment for the NMAFGE experiment include the working face support system and gob-side entry support system. The working face support system mainly includes a hydraulic support system and an exclusive support system. The hydraulic support system is located in the head entry and the middle of the working face, and the exclusive support system is located in the tail of the working face. The exclusive support system includes exclusive transition support, support for the drilling machine and exclusive face-end support. The front toe of the base of the support for the drilling machine is provided by an anchor drilling rig, and the middle platform of the front and rear pillars is provided by a dynamite borehole drilling rig. The gob-side entry support systems include temporary roof-cutting support and constant-resistance and large-deformation anchor (CRLDA) cables. The array spacing of the CRLDA cables is the cut depth of a coal cutter. The top beam of the temporary roof-cutting support is 1800 ×700 mm, and the spacing between adjacent supports is 795 mm.

The process flow is shown in Fig. 2 and is roughly divided into five steps. Step 1 is the formation of the circular arc coal side, which mainly relies on the coal cutter to cut the roadway space on the exclusive scraper conveyor. Step 2 is anchor cable installation because the position of the drilling rig may be different due to constraints on the equipment arrangement space at the tail. Additionally, the roof anchor support cannot be simultaneously constructed in the array. Thus, anchor cables #1 and #3 are constructed first in each section; anchor cable #5 on the side of solid coal lags behind anchor cable #1 by 1 array spacing; anchor cable #4 lags behind anchor cable #1 by 7 array spacings; and anchor cable #2 lags behind anchor cable #1 by 8 array spacings. Step 3 is roof cutting and installation of

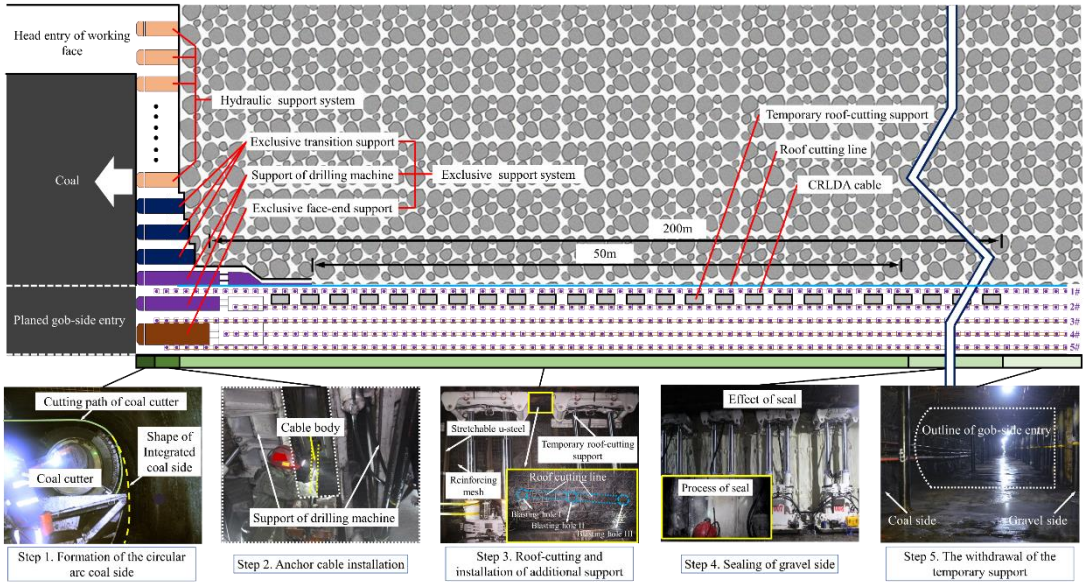

Fig. 2 Main support equipment, system and process flow of the NMAFGE (Liu *et al*. 2019)

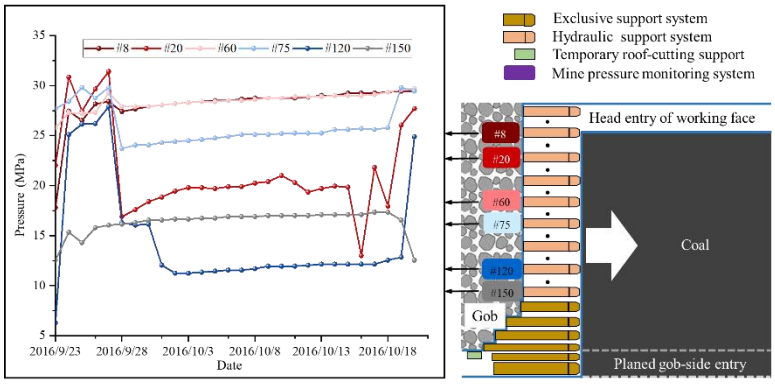

Fig. 3 Mine pressure pattern of the working face (Zhou *et al.* 2019)

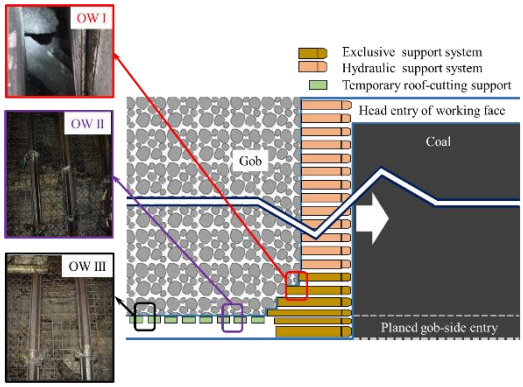

Fig. 4 Visual distribution characteristics of the gangue in the rear of the support

additional support. In the roof-cutting process, explosive blasting construction was carried out multiple times approximately 1 m behind the cutting rig, and the cutting line length and angle were 9 m and 10°, respectively. Unlike traditional roadway support, gob-side entry in NMAFGE practice requires additional support. The additional support includes temporary support and gravel support. The temporary support mainly included temporary roof-cutting support complemented with a hydraulic single pillar and top beam. The gravel support mainly included stretchable U-steel and reinforcing mesh, complemented by lateral support from the temporary roof-cutting support. Step 4 is sealing of the gravel side. Polymer sealing material (with a thickness of 30 ~ 50 mm) was sprayed on the gravel side 50 m from the gangue support baffle behind the working face support of the drilling machine. Step 5 is the withdrawal of the temporary support. The temporary support was withdrawn 200 m behind the end frame of the gob-side

entry. The concrete pillar simple support of the gob-side entry was constrained with ordinary steel pipe.

2.2 Distribution characteristics of the gangue beside the gangue support structure

In the NMAFGE process, the gob roof at the entry retaining side is cut using directional cutting technology, and the suspended roof in the gob gradually caves in response to the mine pressure and its own gravity. As the excavation space advances forward, mining activities cause stress redistribution in the roof rock. In the temporal-spatial evolution process of the roof structure, stress will induce primary crack propagation accompanied by secondary cracking. In the field, this process is mainly reflected by filling of the gob by a gangue composed of crushed roof rock. This work intends to obtain the distribution characteristics during the gangue heaping process in addition to the gangue support structure according to the mine pressure pattern of the working face and the visual distribution characteristics of the gangue in the rear of the support.

The mine pressure pattern of the working face is shown in Fig. 3. To facilitate the analysis, the author collected the data from the hydraulic support pressure device at midnight each day before 2016/10/20. In the mine pressure distribution characteristics, the highest pressure at the working site is mainly distributed around the #8 and #60 hydraulic supports of the working face, and the pressure in the zones around the #150 and #120 hydraulic supports is relatively low. Stress changes lead to changes in roof damage. The mine pressure pattern of the working face implies that the distribution of the gangue in the hydraulic support rear of the working face is characterized by less gangue mass in the gob-side entry and more gangue mass in the zones closer to the middle of the gob.

According to the mine pressure pattern, the distribution of gangue accumulation in the gob is not sufficient. An observation window (OW) for the gangue was provided in the support, and visual analysis of the distribution characteristics of the gangue in the rear of support was performed according to the observation results at different sites. As shown in Fig. 4, the gap between the first exclusive transition support and the second exclusive transition support near the hydraulic support is OW I, the gangue support net between the second temporary roof-cutting support and the third temporary roof-cutting support near the working face is OW II, and the gangue support net between the seventh temporary roof-cutting support and the eighth temporary roof-cutting support near the working face is OW III. It can be observed that the heaping height of the gangue in the OW I zone is the highest, that in the OW II zone is the lowest, and that in the OW III zone is basically the same as the roadway height. The characteristics based on multiple field observations are consistent.

Combined with the analysis of the mine pressure pattern and the visual distribution characteristics of the gangue at the rear of the support, the distribution characteristics of the gangue heaping process beside the gangue support structure can be roughly distributed into a dynamic shock phenomenon and a static stacking phenomenon. The dynamic shock phenomenon occurs in the early stage of the gangue heaping process. This phenomenon occurs because the pressure changes on both sides of the working face lag behind the pressure change in the middle, and the gob-side gangue heap is likely to form a sloping structure. In contrast, static stacking occurs in the late stage of the heaping process of gangue. This phenomenon occurs because the gob-side roof constantly caves in response to the mine pressure and its own weight, and the heaping height of the gangue beside the gangue support structure is constantly increased.

In the dynamic shock phenomenon, the gangue formed by roof caving rolls down the slope and is likely to cause an impact force in the gangue support structure. In the static stacking phenomenon, the gangue support structure is only subject to the lateral extrusion force in the gangue heaping process. Since the characteristics of the impact force in the case of the dynamic shock phenomenon and those of the extrusion force in the case of the static stacking phenomenon are definitely different, these two forces acting on the gangue support structure should be analysed separately.

3. Theoretical analysis

3.1 Analysis of the impact force

To model the dynamic shock phenomenon in the early stage of the gangue heaping process, the plane gangue collision mechanical model is composed of the gob-side gangue heaped at the roof-cutting line side and the gangue support structure. The impulse concept is often used to resolve the action forces (such as impact) between objects in a transient process (Sarfarazi *et al.* 2016; Gao and Meguid 2018; Nakajima *et al.* 2020). Because the internal structure of the slope formed by the heaping of gangue is loose and the rigidity of the gangue is greater than that of the slope (assuming that the gangue clasts are rigid bodies), the collision between gangue clasts when moving down the slope is a rigid collision. The landing point of the gangue is usually at the site where the slope suddenly changes or where the collision velocity of rolling rocks changes (Zheng *et al*. 2012; Asteriou *et al*. 2018). Assuming that the gangue is not subject to air resistance, the motion trajectory after the gangue clasts collide with each other can be approximated as a parabola (Fanos *et al*. 2018; Le Roy *et al*. 2019; Di Luzio *et al*, 2020). The author attempts to introduce the coefficient of restitution to analyse the velocity changes before and after collision and further analyses the force of the gangue acting on the gangue support structure in the case of the dynamic shock phenomenon.

In the plane gangue collision mechanical model, the velocity of the centroid of a gangue clast was observed to analyse how the velocity changes during gangue movement. The motion characteristics are shown in Fig. 5, in which it is assumed that a gangue clast with a mass of m_{GC} falls vertically from a height of h_{Ff} to the landing point on the

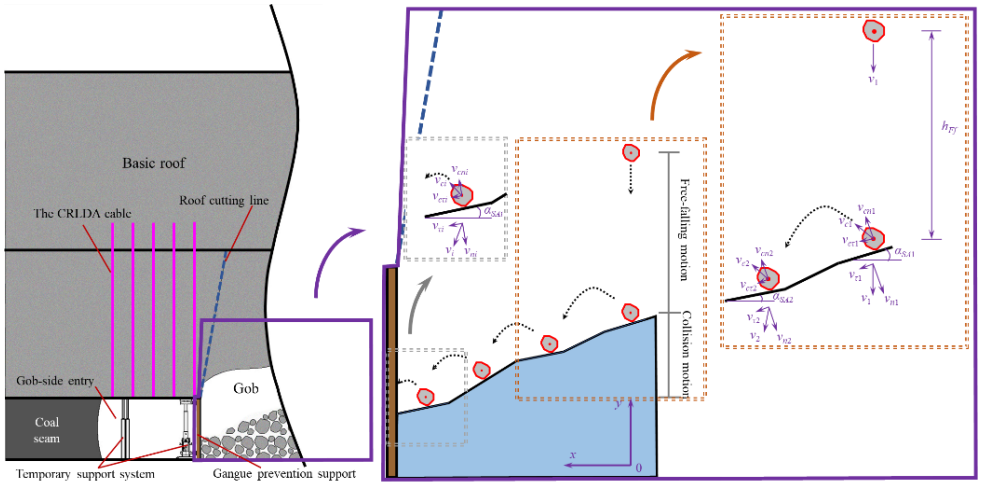

Fig. 5 Diagram of the plane gangue collision mechanical model in the case of the dynamic shock phenomenon

slope. Its movement process involves free fall, i_{th} (i=1~n) collisions between the gangue clast and the slope, and the gangue clast colliding with the gangue support structure. Here, the number of collisions (i_{th}) mainly depends on the distance between the first impact site and the gangue support structure.

When the gangue leaves the roof rock, it freely drops under the action of gravity. Because the effect of air resistance was neglected here, the velocity remained the same during the fall. Thus, the velocity of the gangue clast before collision is v_1, namely,

$$v_1 = \sqrt{2gh_{Ff}} \tag{1}$$

where h_{Ff} is the height of the gangue during free fall and g is the acceleration due to gravity.

Assuming that the gangue directly impacts the gangue support structure after the i_{th} collision, the velocity and slope angle at the i_{th} collision are v_i and α_{SAi}, respectively. Let the initial position of the gangue at the i_{th} oblique projectile motion be (x_{ci}, y_{ci}); the resultant velocity of the tangential velocity (v_{cti}) and the normal velocity (v_{cni}) corresponding to the centroid of the gangue be v_{ci}; and the velocity component of the x-y coordinate axis corresponding to v_{ci} be v_{xci} and v_{yci}, respectively. The velocity of the centroid v_{xyi} when the gangue collides with the gangue support structure in the motion trajectory is as follows:

$$v_{xyi} = \sqrt{e_{ni}^2 v_i^2 \cos^2\alpha_{SAi} + e_{\tau i}^2 v_i^2 \sin^2\alpha_{SAi} + 2g(y_c - y_{ci})} \tag{2}$$

where e_{ni} is the normal coefficient of restitution at the i_{th} collision, $e_{\tau i}$ is the tangential coefficient of restitution at the i_{th} collision, α_{SAi} is the angle between the position of the i_{th} collision and the horizontal plane, and y_c is the height of the gangue in the y direction when colliding with the gangue support structure.

After the gangue collides with the gangue support structure, the impact force continues to act upon the structure for a duration Δt. Based on Eq. (2), the impact force F_{GC} during motion can be expressed as follows:

$$\begin{aligned} F_{GC}\Delta t &= m_{GC} v_{xyi} \\ &= m_{GC}\sqrt{e_{ni}^2 v_i^2 \cos^2\alpha_{SAi} + e_{\tau i}^2 v_i^2 \sin^2\alpha_{SAi} + 2g(y_c - y_{ci})} \end{aligned} \tag{3}$$

The impact force of the gangue is mainly subject to the velocity of the gangue after colliding with the slope. It is assumed that the height of the fall is constant. For a gangue caving directly from the roof on the roof-cutting line side or a gangue caving from the roof on the noncutting side, the velocity of the gangue after each collision is influenced by certain factors, including the coefficient of collision, slope angle, and precollision velocity. However, these factors were random in the field project, leading to random velocities after the collision of the gangue. Therefore, the impact force of the gangue was a random numerical value. The action time of the impact force applied by the gangue was short, and the force applied to the gangue support structure experienced sudden increases and decreases, so the variation trend of the impact force applied by the gangue was disordered.

However, due to the crushing expansion characteristics of the gangue, h_{Ff} will decrease with increasing heaping height, resulting in a decrease in the initial velocity v_1. The velocity also decreases during collisions. If the initial velocity decreases, the final velocity at which the gangue collides with the gangue support structure also decreases. An integrated analysis suggests that in the case of the dynamic shock phenomenon, the variation trend of the impact force of the gangue when colliding with the gangue support structure was disordered, but the impact force decreased with increasing heaping height of the gangue.

3.2 Analysis of the extrusion force

Combined with the static stacking phenomenon in the late gangue heaping phase, as illustrated by the case shown in Fig. 6, the plane gangue extrusion mechanical model was composed of the supplementary gangue, the original height of the gangue heap beside the gangue support structure, and the gangue support structure. Because the gob-side stratum angle was nearly horizontal and given the height of the

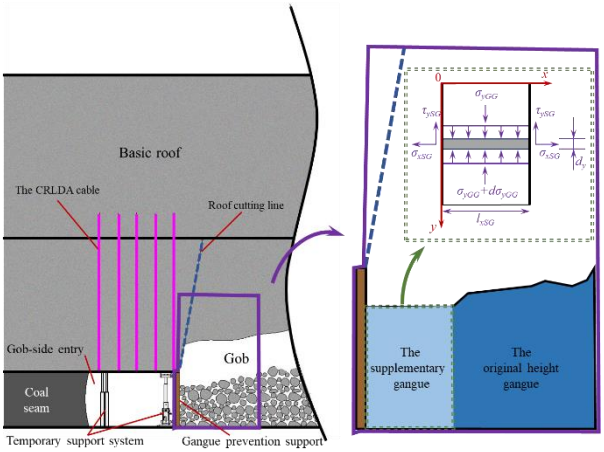

Fig. 6 Diagram of the plane gangue extrusion mechanical model

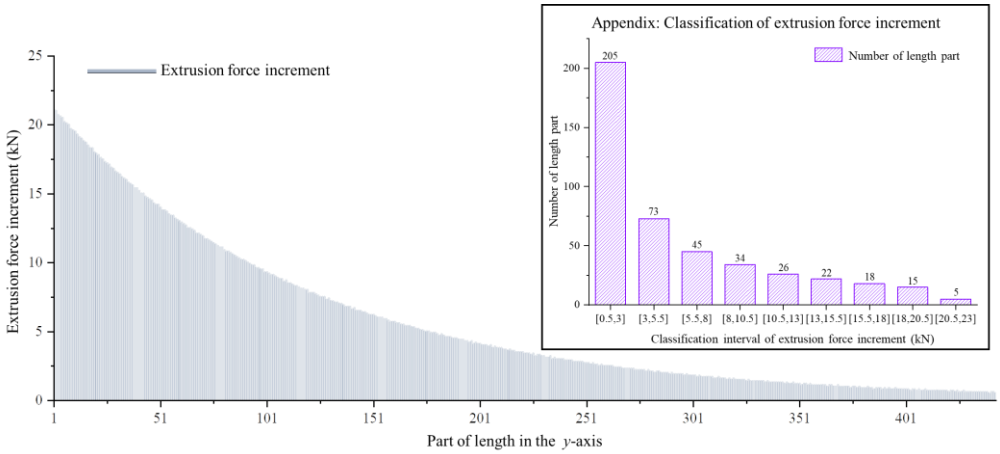

Fig. 7 Variation trend of the extrusion force increment

entire gob, the length of the supplementary gangue clasts was very short. The original height of the gangue heap and the gangue support structure constrained the supplementary gangue from moving to either side. The Janssen model is used to explain the phenomenon in which the bottom pressure in a granary gradually stabilizes with increasing heaping heights of loose objects (Horabik *et al*. 2016, Matchett *et al*. 2018, Cisneros *et al*. 2020, Mahajan *et al*. 2020, Yoon *et al*. 2020, Zidek *et al*. 2020). Furthermore, the plane gangue extrusion mechanical model also satisfies the assumption of the Janssen model—the axial pressure of loose rock is linearly related to its lateral pressure, and the coefficient of friction between the gangue and the gangue support structure is constant. Unlike the method of analysing the lateral stress on the gangue side used in other references (Zhen *et al*. 2019), the author innovatively introduces the Janssen model to analyse the extrusion force of gangue on the gangue support structure in the case of the static stacking phenomenon.

As shown in Fig. 6, in the plane gangue extrusion mechanical model, the x-y coordinate system was set up, and a gangue with a thickness of dy was selected from the supplementary gangue beside the gangue support structure. The vertical height from the gangue with a thickness of dy to the top of the supplementary gangue is y. The pressure of the gangue in the high layer applied to the gangue in this layer is σ_{yGG}, and the pressure of the gangue in this layer applied to the lower gangue is $\sigma_{yGG}+d\sigma_{yGG}$. To maintain mechanical equilibrium, the tangential friction (τ_{ySG}) and the lateral extrusion force (σ_{xSG}) of the supplementary gangue applied to the gangue support structure and the original height gangue were kept the same.

As shown in Fig. 6, a linear first-order differential equation is derived from the vertical force equilibrium on the differential slice of material

$$\frac{d\sigma_{ySG}}{dy}+\frac{2\mu_{GG}K_{GG}\sigma_{ySG}}{l_{xSG}}=\gamma_G \tag{4}$$

where γ_G is the bulk density of the gangue; l_{xSG} is the length of the supplementary gangue, which is mainly associated with the lumpiness of the supplementary gangue; K_{GG} is the ratio of the lateral pressure (σ_{xSG}) to the vertical pressure (σ_{yGG}); and μ_{GG} is the static coefficient of friction between the gangue and the gangue support structure.

According to the Janssen model, the lateral extrusion force (σ_{xSG}) of the supplementary gangue is as follows:

$$\sigma_{xSG}=K_{GG}\sigma_{yGG}=\frac{\gamma_G l_{xSG}}{2\mu_{GG}}\left(1-e^{-2\mu_{GG}K_{GG}y/l_{xSG}}\right) \tag{5}$$

In Eq. (5), γ_G is basically constant. If the contact surface

is extremely rough, μ_{GG} is tan(φ_{IG}), and φ_{IG} is the internal friction angle of gangue. In the plane gangue extrusion mechanical model, if the values of K_{GG} and l_{xSG} are determined, the variable controlling the lateral extrusion force (σ_{xSG}) applied to the gangue support structure is mainly y. Affected by support for the drilling machine, the gangue in this area ultimately fell down. Therefore, l_{xSG} is the width of the rig support, which was 1680 mm. The K_{GG} of the loose gangue can be expressed by the internal friction angle and external friction angle. By combining this information with Fig. 6, an equation for the calculation of K_{GG} can be obtained:

$$K_{GG} = \frac{\cos^2\varphi_{IG}}{1+\sin^2\varphi_{IG}+2\sin\varphi_{IG}\sqrt{[1-\frac{4\left(x-\frac{l_{xSG}}{2}\right)^2(\frac{\tan\varphi_{OG}}{\tan\varphi_{IG}})^2}{{l_{xSG}}^2}]}} \quad (6)$$

where φ_{OG} is the external friction angle of the gangue and φ_{OG} = arctan(μ_{GG}).

In Eq. (6), φ_{IG} is basically constant. The range of x in this equation is 0 to l_{xSG}, and the gangue support structure is exactly at x=0. Therefore, an equation for the calculation of K_{GG} at the gangue support structure can be obtained:

$$K_{GG} = \frac{\cos^2\varphi_{IG}}{1+\sin^2\varphi_{IG}+2\sin\varphi_{IG}\sqrt{[1-(\frac{\mu_{GG}}{\tan\varphi_{IG}})^2]}} \quad (7)$$

To intuitively obtain the change trend of the pressure, the extrusion force increment ($\Delta\sigma_{xSG}$) is analysed. If the length of the y-axis is divided into n parts, then the length of each part can be expressed in terms of y_i(i=1~n). Therefore, an equation for the calculation of $\Delta\sigma_{xSG}$ can be obtained:

$$\Delta\sigma_{xSG} = \sigma_{xSG}(y_{i+1}) - \sigma_{xSG}(y_i) \quad (8)$$

where $\sigma_{xSG}(y_i)$ is the extrusion force at y=y_i and $\sigma_{xSG}(y_{i+1})$ is the extrusion force at y=y_{i+1}.

Combining Eqs (5), (7) and (8), the parameters used to represent the N00 working face of the Ningtiaota Coal Mine are as follows: γ_G= 27×10^3 N/m^3, φ_{IG}=41.33°, and y=0~8.86 m. If μ_{GG} = tan(φ_{IG}). To analyse the extrusion force rate, the length of the y-axis is divided into 443 parts. Thus, the extrusion force increment can be calculated.

The variation trend of the extrusion force increment at the gangue support structure is shown in Fig. 7. As the number of the length part along the y-axis increased, the extrusion force increment ($\Delta\sigma_{xSG}$) gradually decreased until the minimum value was 0.5 kN. As shown in the appendix of Fig. 7, the larger the extrusion force increment value was, the smaller the number of the length part. The largest value was between 0.3 kN and 3 kN at length part number 205. The variation trend of the extrusion force increment can reflect the variation trend of the extrusion force. This may indicate that in the case of the static stacking phenomenon, the extrusion force of the gangue applied to the gangue support structure increased rapidly, then increased slowly, finally approaching a fixed numerical value.

4. Field monitoring

4.1 Description of the monitoring method

To validate the variation patterns of the impact force and the extrusion force applied to the gangue support structure as described in the theoretical analysis, the author attempts to verify the results obtained from the theoretical analysis by field monitoring. Field monitoring of the lateral pressure at the gangue side was conducted with the NMAFGE gangue side lateral pressure monitoring system.

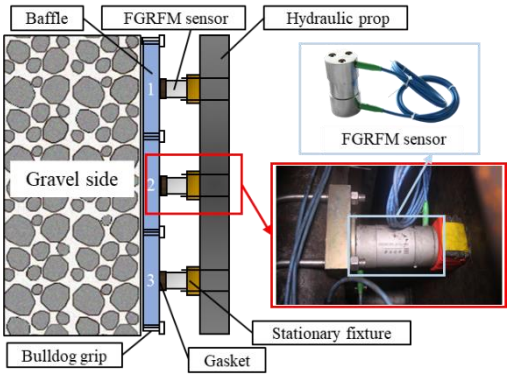

Fig. 8 Profile of the monitoring system

This monitoring system was arranged between two stretchable U-shaped steels and comprised a fibre grating reaction sensor (FGRFM sensor), gasket, stationary fixture, bulldog grip, baffle and hydraulic prop. Fig. 8 shows the profile of the monitoring system. In the first step, 3 baffles were vertically embedded on the metal mesh on the gravel side and then fixed with the bulldog grip. The hydraulic prop was adjusted to the design position and height, and the stationary fixture was securely mounted at the design position of the hydraulic prop. The FGRFM sensor was loaded onto the stationary fixture, and the gasket was mounted between the FGRFM sensor and baffle to ensure that the FGRFM sensor, baffle and hydraulic prop were in close contact with each other. However, this monitoring system had one drawback. Because the baffle at each monitoring point hung on the metal mesh on the gangue side, the force was effectively transmitted through the metal mesh. This was indicated by the simultaneous increases or decreases at the three monitoring points, but the largest change at a given monitoring point was most directly affected by the force.

For convenient acquisition of the monitoring data, reasonable monitoring points were selected, cleaned and levelled. The monitoring system was deployed immediately after the gangue support structure was installed. In this monitoring scheme, two monitoring stations were arranged at the gob-side entry. As shown in Fig. 9, Monitoring Station 1 was arranged 30 m from the beginning of the gob-side entry, and Monitoring Station II was arranged 50 m from the beginning of the gob-side entry. Considering that part of the area on the gravel side was occupied by the lateral pressure plate of the roof-cutting support, 3 baffles were arranged in the remaining space at each monitoring station, and 2 FGRFM sensors were placed on each baffle. The #1 and #2 FGRFM sensors were arranged 2500 mm from the floor of the entry, the #3 and #4 FGRFM sensors were arranged 1500 mm from the floor of the entry, and the #5 and #6 FGRFM sensors were arranged 500 mm from the floor of the entry. The array spacing of the FGRFM sensors

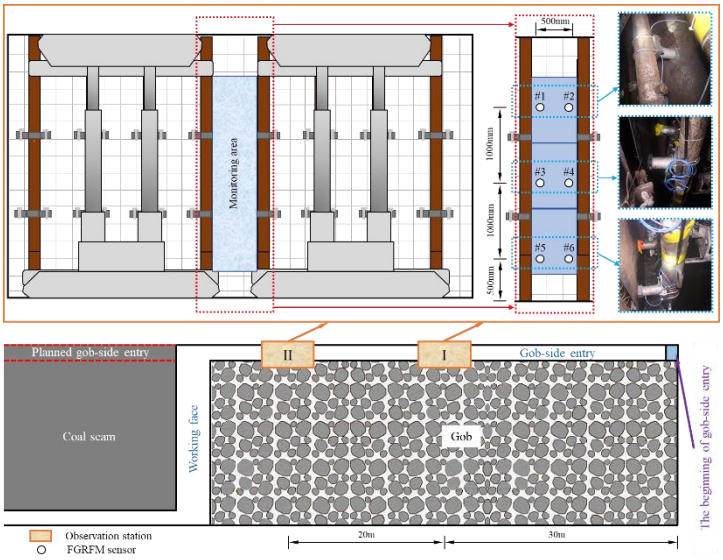

Fig. 9 Diagram of the arrangement of monitoring stations

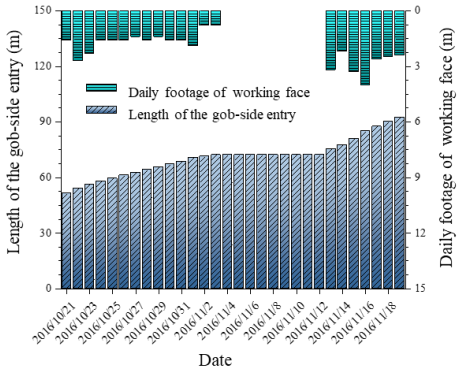

Fig. 10 Diagram of the gob-side entry length and daily footage of the working face

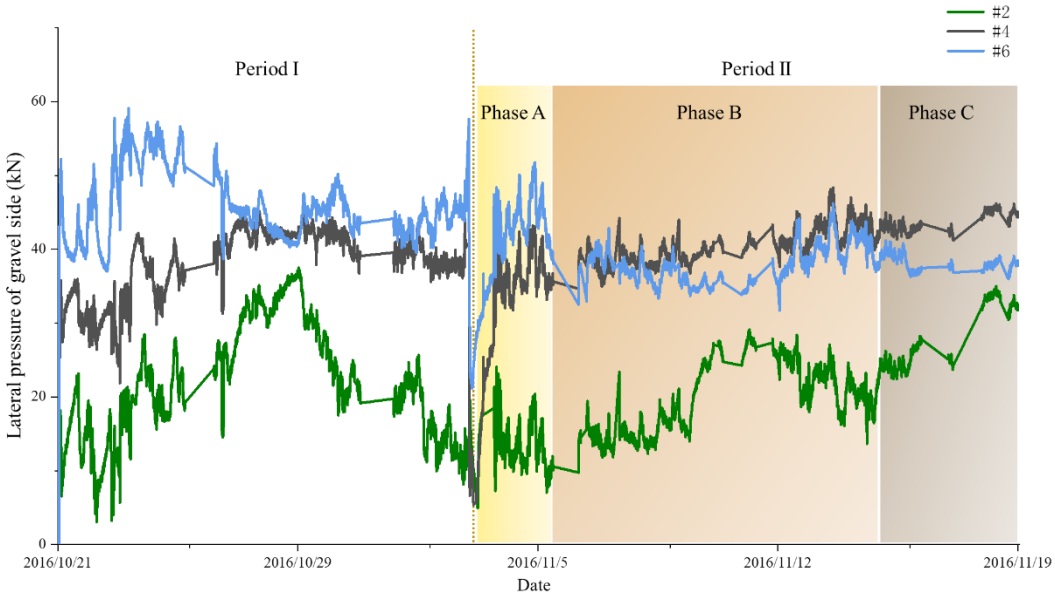

Fig. 11 Lateral pressure on the gangue side

was set to 500 mm. The FGRFM sensors acquired data at an interval of 5 mins.

The rapid advancement of the working face certainly accelerates the change in the overall mine pressure. To

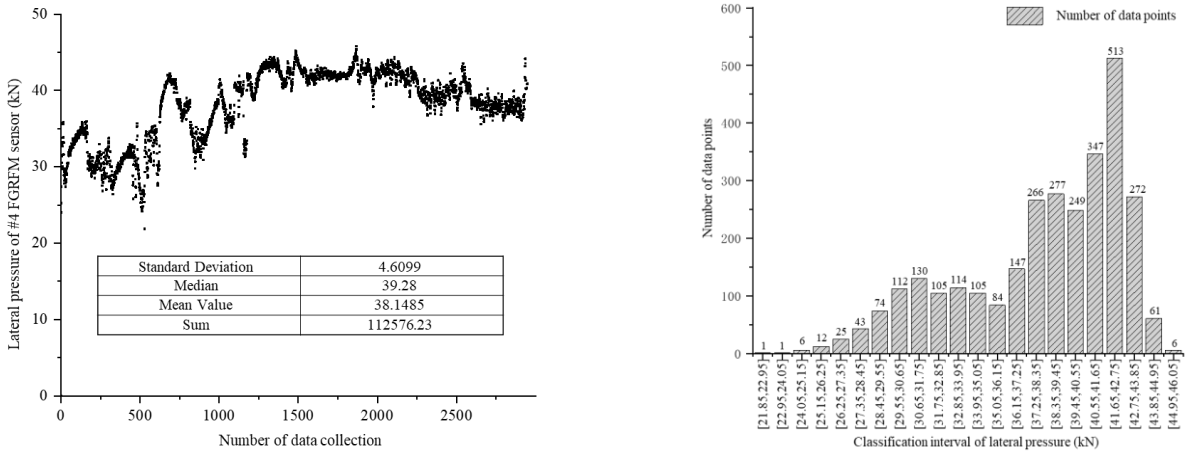

(a) Descriptive statistics (b) Classification statistics

Fig. 12 Lateral pressure analysis in Period I at Monitoring Point #4

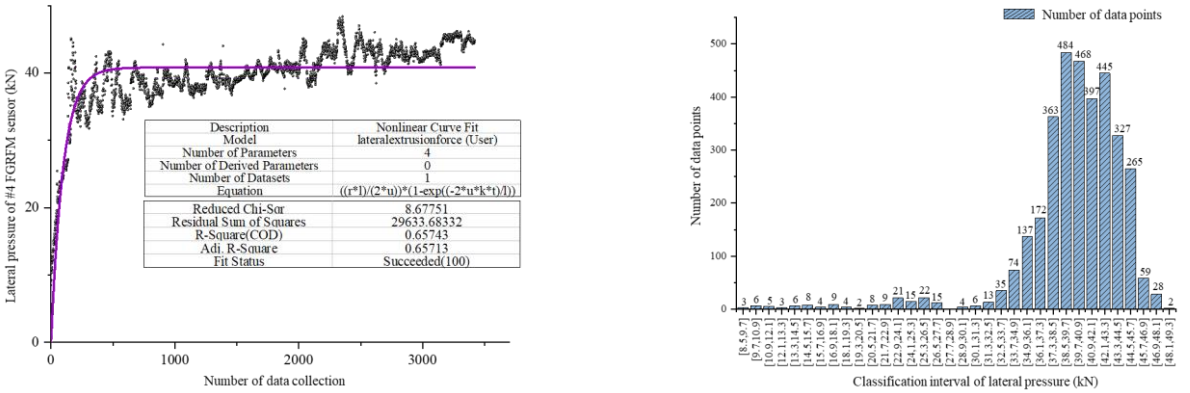

(a) Descriptive statistics (b) Classification statistics

Fig. 13 Lateral pressure analysis in Period II at Monitoring Point #4

obtain more data before the first weighting of the roof, the drilled footage in the working face per day should be greatly reduced. As shown in Fig. 10, the drilled footage per day was approximately 1.42 m, further guaranteeing that it would take 30 days to increase the length of the gob-side entry from 50 m to 92.5 m. In this study, FGRFM sensor data before 2016/11/19 were selected for analysis.

4.2 Analysis of the monitoring results

The variation trends in the data collected from the 12 FGRFM sensors at the two monitoring stations in the monitoring system were similar. For the convenience of analysis, the data collected from the #2, #4 and #6 FGRFM sensors at Monitoring Station II are interpreted in this section. The curve shown in Fig. 11 is the variation trend of the numerical lateral pressure value on the gangue side.

From the monitoring results, by setting the minimum numerical values of the monitoring data as the limits, the curve of the lateral pressure gravel side can be roughly divided into two periods. Period I involves the data collected from 2016/10/21 to 2016/11/2, and Period II involves the data collected from 2016/11/3 to 2016/11/19.

The data collected in Period I were more disordered and subject to sudden increases and decreases until finally decreasing to a minimum, indicating that every monitoring point was subject to the impact force associated with the dynamic shock phenomenon during most of this period. The peaks in the data obtained at Monitoring Points #6, #4, and #2 were 59.09 kN (2016/10/23), 45.18 kN (2016/10/27), and 37.51 kN (2016/10/29), respectively, which in turn verify that the impact force in the case of the dynamic shock phenomenon decreased with increasing heaping height of the gangue.

Based on the different variation trends in the monitoring results, the data obtained in Period II can also be divided into three phases, and the change characteristics of the three phases are similar to those of the phase of the extrusion force. However, the characteristics of the monitoring points in the high position lag behind those in the low position. In Phase A, the variation and numerical values of the data were larger than those in the other phases. In Phase B, the data variation trends at the monitoring points were relatively gradual. In Phase C, the data variations at the monitoring points were very small and gradually approached a fixed numerical value. The final numerical values at Monitoring Points #2, #4, and #6 were 31.91 kN, 44.82 kN and 38.19 kN, respectively, indicating that the final numerical values approached by the final extrusion force were independent of the gangue height and that the

force applied by the gangue at different positions did not vary greatly.

To increase the scientific nature of the analysis results, data from measurement point #4 were taken separately for analysis. Therefore, according to the characteristics of the changes in different periods, the data were analysed mathematically using statistics. To facilitate the analysis, the number of collected data points was used as the variable instead of the date.

As shown in Fig. 12 (a), by calculating the standard deviation, mean value, median and sum of the data, it can be concluded that the change in this group of data is chaotic. The most intuitive attribute was that the standard deviation was 4.6099. The classification statistics except for the initial point (0 kN) are shown in Fig. 12 (b). By classifying the lateral pressure, it can be concluded that most of the points were concentrated in the interval with high pressure values. Among these points, the largest point number with a value between 41.65 kN and 42.75 kN was 513. Through mathematical statistics, it can be concluded that the change in lateral pressure in this period was chaotic, but the value of stress was generally large. The force change characteristic agrees with the analysis result of the impact force.

In Period II, the fitting analysis results are shown in Fig. 13 (a), and the data from Monitoring Point #4 had a high fitting degree with the calculation formula of lateral stress. The R-squared value (COD) was 0.65743, and the fit status indicated success (100). The classification statistics are shown in Fig. 13 (b), and it can be concluded that most of the points were concentrated in the interval with high pressure values. There were many intervals that contained large numbers of data points, such as [37.3,38.5], [38.5,39.7] and [42.1,43.3]. Unlike the data in Period I, the lateral pressure in Period II usually increased gradually from small to large, rather than mainly remaining concentrated in the range of large lateral forces. An integrated analysis suggested that the data variation trend in Period II exhibited a sharp increase, a slow increase, and a steady state.

In summary, in the heaping process of the gangue, the bottom part of the gangue support structure was first subjected to the highest impact force, and the variation trend of the impact force on the whole gangue support structure was chaotic. The extrusion force of the gangue applied to the gangue support structure first increased rapidly, then increased slowly, and finally approached a fixed value. The final extrusion force was unrelated to the gangue height, and the force applied by the gangue at different positions did not vary greatly.

5. Discussion

In the NMAFGE experiment, previous work analysed only the force applied to the gangue support structure during gangue compaction and did not analyse the force change characteristics of the gangue support structure during gangue heaping. If the stability of the gangue support structure cannot be maintained in the heaping process of gob-side gangue, the stability of the entry will definitely be affected.

The force change of the gravel side support during gangue heaping is studied in this paper in five stages: research question, research objective, theoretical study, field observation and summary. The flow chart of the method described in this paper is shown in Fig. 14. According to the mine pressure pattern and field monitoring results, the distribution characteristics of the gangue during the heaping of the gob-side gangue and the gangue support structure can be roughly divided into a dynamic shock phenomenon and a static stacking phenomenon. According to the distribution characteristics of the gangue, the force of the gangue support structure can be divided into an impact force and an extrusion force. For theoretical analysis and field monitoring, the variation characteristics of the impact force and extrusion pressure were basically obtained. In the NMAFGE experiment, considering the evolution pattern of the force of the gangue acting on the gangue support structure, the stability on the gangue side should be studied. After summarizing the variation characteristics of the force, the following conclusions were preliminarily obtained: more attention should be given to monitoring the offset at the bottom of the gangue support structure in the initial heaping phase, and slipping of the gangue support structure due to the global force should be prevented in the late heaping phase, as it may affect the stability of the entry. To validate the rationality of this work, along with the monitoring study of the lateral stress on the gangue side, the author conducted a field observation of the deformation of the gangue support structure. The image data of the deformation of the gangue support structure on the gangue side in the NMAFGE experiment were collected during the field observation.

The deformation types of the gangue support structure at the gangue side are shown in Fig. 15. Based on the comparison of many images, the author divided the deformation types of the gangue support structure at the gangue support into the bottom offset and overall slip. The bottom offset is shown in Fig. 15(a). The offset angles of the stretchable U-steel and reinforcing mesh near the bottom of the entry were high. This phenomenon demonstrates that the impact force in the case of the dynamic shock phenomenon decreases with increasing height. The overall slip is shown in Fig. 15(b). The whole gangue support structure is flat, but the whole gangue support structure has moved towards the entry. For example, the distance from the gangue support structure to the first steel belt of the CRLDA cable continued to decrease from the initial distance of 0.5 m, and more seriously, the gangue support structure eventually extended beyond the position of the first steel belt of the CRLDA cable. This phenomenon demonstrates that the gangue can jointly extrude the gangue support structure at a constant force, resulting in slipping of the whole gangue support structure. The analysis results based on the image data demonstrate that the theoretical analysis and the field monitoring results are reasonable.

The analysis results of the force of the gangue acting upon the gangue support structure provide a scientific

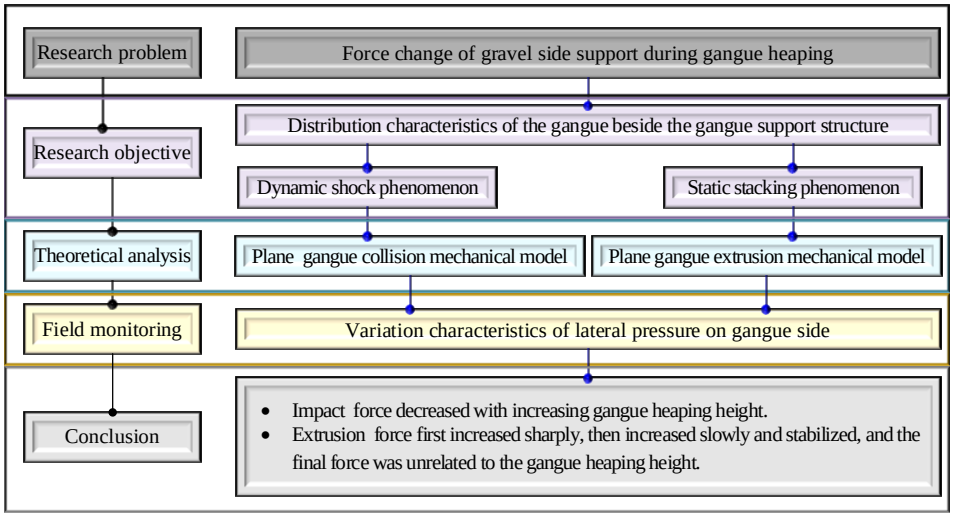

Fig. 14 Analysis flow chart of the force change of the gravel side support during gangue heaping

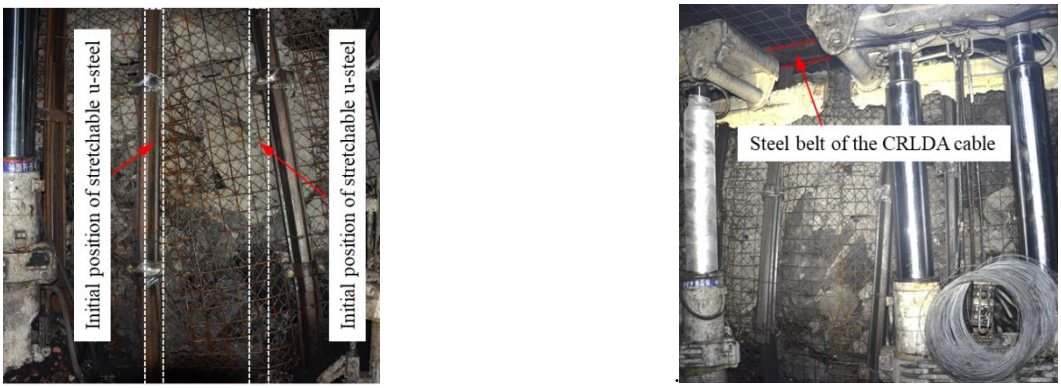

(a) Bottom offset (b) Overall slip

Fig. 15 Deformation types of the gangue support structure at the gangue side

reference for the study of the stability of the gangue side in future NMAFGE experiments; however, this research method remains subject to certain limitations. For example, the project background in which this work was set is relatively simple, featuring a shallow burial depth of the coal seam, a nearly horizontal stratum, and no special geological structures. In the mining process of a coal seam with a large dip angle, the slope angle formed by the gangue is bound to be different from that near a horizontal coal seam. If future NMAFGE experiments are carried out for coal seams with larger dip angles, the coal seam inclination should be considered in the impact force analysis method. The stress environment of coal seams in deep mining is dominated by horizontal stress, and the characteristics of lateral extrusion of the gangue in this stress environment must be different from those for coal seams in shallow mining. The stress environment in special geological structures such as different faults or collapse columns where coal seams are located is also different from that under simple geological conditions. Future research should focus on complex geological conditions, and more research efforts should be undertaken. For the impact force and extrusion force, the author considered that the force applied to the gangue support structure varies with different degrees of lumpiness of the gangue. At the same time, the contact mode between gangues is also an area that has not been considered in the current research methods. Future research will further include the lumpiness and contact mode of the gangue in the field monitoring process. For example, transparent baffle material will be developed for use in the monitoring system, gangue lumpiness and contact mode data will be collected while obtaining the force applied to the gangue support structure, and a detailed analysis will be performed on the variation characteristics of the force applied to the gangue support structure.

6. Conclusions

In the NMAFGE experiment, the distribution characteristics of the gob-side gangue in the heaping process are roughly divided into a dynamic shock phenomenon and a static stacking phenomenon. In the case of the dynamic shock phenomenon, the gangue exerts an impact force on the gangue support structure, and in the case of the static stacking phenomenon, the gangue exerts a horizontal extrusion force on the gangue support structure.

For the impact force, the results of the theoretical

analysis indicate that the variation trend of the impact force is disordered, but the impact force decreases with increasing heaping heights of the gangue. For the extrusion force, the results of the theoretical analysis indicate that the variation trend of the extrusion force exhibits a sharp increase followed by a slow increase and finally stabilizes, and the extrusion force is unrelated to the heaping height of the gangue.

In the field monitoring study of the lateral stress of the gangue support structure, the monitoring results were divided into two periods according to different variation patterns of the lateral force applied on the gangue side. In Period I, the overall data variation trend was disordered, but the peak value of the data obtained from the monitoring point at a lower height was greater than that at any other monitoring point. For instance, the peaks in the data collected from Monitoring Points #6, #4 and #2 were 59.09 kN (2016/10/23), 45.18 kN (2016/10/27), and 37.51 kN (2016/10/29), respectively. In Period II, the data obtained from the monitoring points exhibited a phase of rapid increase, a phase of slow increase and a phase of stabilization. The values reached by the final extrusion force were not related to the gangue height. The final values at #2, #4, and #6 were 31.91 kN, 44.82 kN and 38.19 kN, respectively. The results of field monitoring are similar to the results of the extrusion force analysis.

In NMAFGE experiments, because of the evolution pattern of the gangue forces acting on the gangue support structure, more attention should be given to monitoring the offset at the bottom of the gangue support structure in the initial heaping phase, and overall slipping of the gangue support structure should be prevented in the late heaping phase. These findings provide a reasonable reference for the selection of monitoring points on the gangue side and for stability studies in future NMAFGE experiments.

Acknowledgments

This work is supported by the Foundation for the Opening of State Key Laboratory for Geomechanics & Deep Underground Engineering (SKLGDUEK2024), the National Key R&D Program (No. 2016YFC0600900), the National Natural Science Foundation of China (No. 51904207, 51674265) and China Scholarship Council (CSC NO. 202006430081), which are gratefully acknowledged.

References

Asteriou, P. and Tsiambaos, G. (2018), "Effect of impact velocity, block mass and hardness on the coefficients of restitution for rockfall analysis", *Int. J. Rock Mech. Min. Sci.*, **106**, 41-50. https://doi.org/10.1016/j.ijrmms.2018.04.001.

Nakajima, S., Abe, K., Shinoda, M., Abe, K., Shinoda, M., Nakamura, S. and Nakamura, H. (2020), "Experimental study on impact force due to collision of rockfall and sliding soil mass caused by seismic slope failure", *Landslide*, **18**(1), 195-216. https://doi.org/10.1007/s10346-020-01461-z.

Cisneros, L.A.T., Marzulli, V., Windows-Yule, C. R. K.and Poeschel, T. (2020), "Impact in granular matter: Force at the base of a container made with one movable wall", *Phys. Rev. E*, **102**(1), 012903. https://doi.org/10.1103/PhysRevE.102.012903.

Di Luzio, E.,Mazzanti, P., Brunetti, A. and Baleani, M. (2020), "Assessment of tectonic-controlled rock fall processes threatening the ancient Appia route at the Aurunci Mountain pass (central Italy)", *Nat. Hazards*, **102**(3), 909-937. https://doi.org/10.1007/s11069-020-03939-4.

Fanos, A.M., Pradhan, B., Mansor, S., Yusoff, Z.M.. and bin Abdullah, A.F. (2018) "A hybrid model using machine learning methods and GIS for potential rockfall source identification from airborne laser scanning data", *Landslides*, **15**(9), 1833-1850. https://doi.org/ 10.1007/s10346-018-0990-4.

Gao, G. and Meguid, M. (2018), "Modeling the impact of a falling rock cluster on rigid structures", *J. Eng. Mech.*, **18**(2), 04017141. https://doi.org/10.1061/(ASCE)GM.1943-5622.0001045.

He, M.C., Guo, P.F., Chen, S.Y., Gao, Y.B. and Wang Y.J. (2017), "Supporting technology of roadside in gob-side entry in 110 longwall mining method", *AIP Conf. Proc.*, **1839**, 020020. https:// doi.org/10.1063/1.4982385.

He, M.C., Wang, Q. and Wu, Q.Y. (2021), "Innovation and future of mining rock mechanics", *J. Rock Mech. Geotech. Eng.*, **13**, 1-21. https://doi.org/10.1016/j.jrmge.2020.11.005.

Horabik, J., Parafiniuk, P. and Molenda, M. (2016), "Experiments and discrete element method simulations of distribution of static load of grain bedding at bottom of shallow model silo", *Biosyst. Eng.*, **149**, 60-71. https://doi.org/10.1016/j.biosystemseng.2016.06.012.

Hosseini, N. (2017). "Evaluation of the rockburst potential in longwall coal mining using passive seismic velocity tomography and image subtraction technique", *J. Seismol.*, **21**(5), 1101-1110. https://doi.org/10.1007/s10950-017-9654-4.

Hu, J.Z., He, M.C., Wang, J. Ma, Z.M., Wang Y.J. and Zhang, X.Y. (2019). "Key parameters of roof cutting of gob-side entry retaining in a deep inclined thick coal seam with hard roof." *Energies*, **12**, 934. https://doi.org/ 10.3390/en12050934.

Konicek, P. and Schreiber, J. (2018). "Heavy rockbursts due to longwall mining near protective pillars: A case study", *Int. J. Min. Sci. Technol.*, **28**(5), 799-805. https://doi.org/10.1016/j.ijmst.2018.08.010.

Le Roy, G., Helmstetter, A., Amitrano, D., Guyoton, F. and Le Roux-Mallouf, R. (2019), "Seismic analysis of the detachment and impact phases of a rockfall and application for estimating rockfall volume and free-fall height", *J. Geophys. Res.*, **124**(11), 2602-2622. https://doi.org/10.1029/ 2019JF004999.

Liu, H.F., Zhang, J.X., Li, B.Y., Zhou, N., Li D.Q., Zhang, L.B. and Xiao X. (2021), "Long term leaching behavior of arsenic from cementzed paste backfill made of construction and demolition waste: Experimental and numerical simulation studies", *J. Hazard. Mater.*, **416**, 125813. https://doi.org/10.1016/j.jhazmat.2021.125813.

Liu, J.N., He, M.C., Wang, Y.J., Huang, R.F., Yang, J., Tian, X.C., Ming, C. and Guo S. (2019), "Stability analysis and monitoring method for the key block structure of the basic roof of noncoal pillar mining with automatically formed gob-side entry", *Adv. Civ. Eng.*, 5347683. https://doi.org/10.1155/2019/5347683.

Mahajan, S., Tennenbaum, M., Pathak, S.N., Baxter, D., Fan, X.C., Padilla, P., Anderson, C., Fernandez-Nieves, A. and Ciamarra, M.P. (2020), "Reverse Janssen Effect in Narrow Granular Columns", *Phys. Rev. Lett.* **124**(12), 128002. https://doi.org/ 10.1103/PhysRevLett.124.128002.

Matchett, A.J., Langston, P.A. and McGlinchey, D. (2018), "A model for stresses in a circular silo with an off-centre circular core, using the concept of a principal stress cap: Solution for a completely filled silo and comparison with Janssen and DEM data", *Chem. Eng. Res. Des.*, **129**, 412-414. https://doi.org/ 10.1016/j.cherd.2017.11.029.

Sarfarazi, V., Haeri, H. and Khaloo, A. (2016), "The effect of non-

persistent joints on sliding direction of rock slopes", *Comput. Concrete*, **17**(6), 723-737. https://doi.org/ 10.12989/cac.2016.17.6.723.

Tan, Y.L., Ma, Q., Zhao, Z.H., Gu, Q.H., Fan, D.Y., Song S.L. and Huang, D. (2019), "Cooperative bearing behaviors of roadside support and surrounding rocks along gob-side", *Geomech. Eng.*, **18**(4), 439-448. https://doi.org/10.12989/gae.2019.18.4.439.

Wojtecki, A., Mendecki, M.J. and Zuberek, W.M. (2016). "The seismic source parameters of tremors provoked by destress blastings in coal seam", *J. Min. Sci.*, **52**(2), 258-264. https://doi.org/ 10.1134/S1062739116020382.

Yang, H.Y., Liu, Y.B., Cao, S.G., Pan, R.K., Wang, H., Li Y. and Luo F. (2020), "A caving self-stabilization bearing structure of advancing cutting roof for gob-side entry retaining with hard roof stratum", *Geomech. Eng.*, **21**(1), 23-33. https://doi.org/10.12989/gae.2020.21.1.023.

Yoon, J., Ban, H., Hwang, Y. and Park, D. (2020), "Mitigation method of rockfall hazard on rock slope using large-scale field tests and numerical simulations", *Adv. Civ. Eng.*, 3610651. https://doi.org/10.1155/2020/3610651.

Zhang, C., Canbulat, I., Hebblewhite, B. and Ward, C.R. (2017), "Assessing coal burst phenomena in mining and insights into directions for future research", *Int. J. Coal Geol*. **179**, 28-44. https://doi.org/ 10.1016/j.coal.2017.05.011.

Zhang, X.Y., He, M.C., Yang. J., Wang, E.Y., Zhang, J.B. and Sun, Y. (2020), "An innovative non-pillar coal-mining technology with automatically formed entry: A case study", *Engineering*, **6**, 1315-1329, https://doi.org/10.1016/j.eng.2020.01.014.

Zhang, Z.Y., Shimada, H., Qian, D.Y. and Sasaoka, T. (2015), "Application of the retained gob-side gateroad in a deep underground coalmine", *Int. J. Min. Reclam. Env.*, **30**(5), 371-389. http://doi.org/ 10.1080/17480930.2015.1093729.

Zhen, E.Z., Gao, Y.B., Wang, Y.J and Wang, S. (2019), "Comparative study on two types of nonpillar mining techniques by roof cutting and by filling artificial materials", *Adv. Civ. Eng.* https://doi.org/10.1155/2019/5267240.

Zheng L., Chen, G.Q., Zen, K. and Kasama, K. (2012), "Numerical validation of multiplex acceleration model for earthquake induced landslides", *Geomech. Eng.*, **4**(1), 39-53. https://doi.org/10.12989/gae. 2012.4.1.039.

Zidek, M., Zegzulka, J., Jezerska, L., Rozbroj, J., Gelnar, D. and Necas, J. (2020), "Simulation model of loading bin bottom by bulk material", *Chem. Eng. Res. Des.*, **154**, 151-161. https://doi.org/10.1016/j.cherd.2019.12.008.

Zhou, P., Wang Y., Zhu G. and Gao Y. (2019), "Comparative analysis of the mine pressure at non-pillar longwall mining by roof cutting and traditional longwall mining", *J. Geophys. Eng.*, **16**, 423-438.

CC